

Wiener-Haar Expansion of Stochastic Limit Cycles

Chris L. Pettit¹, Philip S. Beran¹

Summary

Monte Carlo simulation was used to analyze the aeroelastic response of a two degree-of-freedom airfoil with variable pitch stiffness. Structural parameters were chosen to permit the development of limit cycles. When the Monte Carlo results were projected onto a Wiener-Hermite expansion, the resulting simulated realizations of limit cycles exhibited a characteristic energy loss at large times. A sinusoidal model problem was constructed and analyzed to clarify the issues responsible for the poor large-time inaccuracy of the expansion. It was observed that the increasing nonlinearity of the process in the random dimension causes any expansion in terms of global basis functions to collapse over a simulation time of sufficient duration. The recently developed Wiener-Haar expansion was found to almost entirely eliminate the loss of energy at large times.

Introduction

Basic probabilistic methods for linear systems have been employed in gust analysis for several decades, but probabilistic study of aeroelastic stability is a more recent development. Standard gust analysis assumes variability only in the gust velocity and depends on linear structural dynamics to develop equivalent static design loads; thus, gust analysis forces an inherently probabilistic process to conform to our deterministic engineering philosophy. In contrast, recent research is the outgrowth of a more holistic perspective on the role of uncertain system and environment properties in establishing the probability of aeroelastic stability. This approach can produce insight in all aeroelastic stability studies, but the payoff likely will be greatest in analyzing the time-dependent behavior of nonlinear systems owing to their generally higher sensitivity [1,2].

The current paper examines a canonical nonlinear aeroelastic system with uncertainty. Monte Carlo simulation (MCS), and stochastic expansions are applied to the study of airfoil limit-cycle oscillation (LCO), which results from a subcritical Hopf bifurcation induced by a nonlinear spring in the pitch degree-of-freedom (DOF). The stochastic expansions employed here involve polynomial chaos expansions (PCE) of the response. The associated theory is summarized in the following section, after which the PCE is applied to the nonlinear airfoil model. Although the PCE accurately represents the short-term stochasticity under post-critical operating

¹Air Vehicles Directorate, Air Force Research Laboratory, Wright-Patterson AFB, OH, 45433, USA

conditions, an unavoidable loss of energy occurs at large times. A simple example based on a sinusoid with random frequency is then discussed to demonstrate that the most commonly employed PCE, the Wiener-Hermite expansion, should be expected to perform poorly for time-accurate modeling of periodic processes.

We demonstrate a way to overcome the loss of energy in PCE-based simulation of limit cycles. The Wiener-Haar expansion [3] is used instead of global (e.g., Hermite or Legendre) basis functions in the random dimension to provide a localized representation of the stochastic process's temporal evolution. We show that the efficacy of this wavelet-based expansion follows from its ability to localize the continually increasing nonlinearity of the process in the random dimension.

Wiener Expansions of Stochastic Processes

Only essential aspects of stochastic expansions are presented here because of space constraints. More details can be found in LeMaître, et al. [3], Pettit and Beran [4], and the references cited therein. We assume θ is an outcome in a probability space, $\xi(\theta)$ is a random variable (rv) that maps outcomes from the probability space to \mathbb{R} , and $y \in \mathbb{R}$ is a possible value of ξ . The rv $\xi(\theta)$ is assumed to be a random system property and $x(t, \xi(\theta))$, a stochastic process, is the associated response. Only processes that depend on a single rv are considered here; LeMaître, et al. [3] summarize the multidimensional generalization.

A general Wiener expansion of $x(t, \xi(\theta))$ can be written as

$$x(t, \xi(\theta)) = \sum_{j \in J} \hat{x}_j(t) \Psi_j(\xi(\theta)) \quad (1)$$

where $\{\Psi_j(\xi(\theta))\}$ is a set of basis functions that are orthogonal with respect to the distribution of ξ and J is an index set whose structure depends on the type of basis. If a spectral expansion is performed, J is one-dimensional; for a wavelet expansion, J is two-dimensional. The Wiener-Hermite (WHe) and Wiener-Legendre (WLe) expansions are examples of the spectral approach. WHe is employed when ξ is a Gaussian rv and WLe is used for a uniform rv. In each case, some scaling of the rv is necessary to match the canonical form of the associated density function. The Wiener-Haar (WHa) expansion is the most elementary example of the wavelet-based approach. It represents a stochastic extension of the well-known Haar wavelet series, in which the orthogonal basis comprises scaled and translated versions of a piecewise constant, compactly supported "mother" wavelet; viz.,

$$\psi(z) = \begin{cases} 1 & 0 \leq z < 1/2 \\ -1 & 1/2 \leq z < 1 \\ 0 & \text{otherwise} \end{cases} ; \quad \psi_k^{(j)}(z) = 2^{j/2} \psi(2^j z - k), \quad j, k \in \mathbb{Z}, \quad (2)$$

where we assume z is a uniform rv on $[0, 1]$. LeMaître, et al. [3] should be consulted for a complete discussion.

Equation (1) is a generalized Fourier series in the random dimension of the process. The coefficients encode the temporal behavior and can be solved for at each time step by enforcing the orthogonality of the basis functions; that is,

$$\hat{x}_j(t) = \frac{\langle x \Psi_j \rangle}{\langle \Psi_j^2 \rangle} \quad (3)$$

where $\langle \cdot \rangle$ denotes the expected value operator, which defines orthogonality of random functions. The denominator, which is the mean-square value of the basis function in question, generally can be tabulated; hence, only the numerator is problem-dependent. Once the expansion coefficients have been evaluated, the stochastic process can be simulated by sampling the random system parameter.

Spectral Projection of LCO on Wiener Bases

Pettit and Beran [2] performed Monte Carlo simulation (MCS) of the airfoil depicted in Figure 1. The unsteady aerodynamics were modeled with the R.T. Jones approximation of the circulatory lift. Parametric variability was included in the third- and fifth-order coefficients of the nonlinear pitch spring, $K_\alpha (\alpha + k_{\alpha_3} \alpha^3 + k_{\alpha_5} \alpha^5)$. The mean value of k_{α_3} was negative to induce a subcritical Hopf bifurcation. The current results include Gaussian randomness only in k_{α_3} . Figure 2 shows the pitch response of the baseline system, which yields a strong LCO.

The MCS time histories were used to evaluate the numerator of Eqn. (3). Then simulated realizations were generated to evaluate the quality of the spectral expansions. Pettit and Beran [4] provide a detailed discussion of the results, which were generally poor. Figures 3 and 4 illustrate this for the third- and tenth-order WHe expansions. Although the early portions of the process are approximated well by spectral expansions, a characteristic loss of energy occurs at large times. This decay is only partially eliminated by increasing the expansion order, but this also leads to spurious amplitude oscillations. (Figure 4).

The source of the WHe projection's inability to encode the long-term pitch oscillations lies in the increasing nonlinearity of the process in the random dimension. We illustrate this through a simple model problem, which involves a sinusoidal stochastic process, $\sin \omega(\xi)t$, whose frequency is a random variable. Both normal and uniform distributions were assumed for ξ . Fifty realizations from $t = 0$ to $t = 3$ are shown in Figure 5 to indicate the evolution of this non-stationary process's distribution over time. Figure 6 illustrates how this process becomes increasingly nonlinear and oscillatory in the random dimension as time progresses. Polynomial

expansions are poorly adapted to approximating highly oscillatory functions, and Figure 7 shows how the WLe expansion fails to capture the long-term behavior of the sinusoidal process; moreover, the realizations show some variability in their extreme value, so that the amplitude is also represented only approximately. Pettit and Beran [4] show that this variability decreases as the size of the original MCS population increases.

Projection of Sinusoidal Stochastic Process on Wiener-Haar Basis

The authors hypothesized that the WHa expansion would be better suited to representing the complex random behavior of this process. The localization of behavior across multiple scales should allow the increasing frequency in the random domain (Fig. 6) to be represented with sufficient accuracy. The sinusoidal model problem was expanded in terms of the Haar basis for a uniformly distributed frequency, $\omega(z)$. Various wavelet resolution levels were evaluated to assess the expansion's resulting quality. Figure 8 shows three realizations of the WHa expansion with six resolution levels (i.e., $J = \max(j) = 5$). Although some variance remains in the simulated amplitude, the long-term decay has been substantially eliminated. Close examination of the associated phase plane plots (not shown here) indicates an amplitude decay on the order of one percent over ten mean periods.

Figure 9 shows how the WHa expansion approximates the process at $t = 9$; both $J = 5$ and $J = 6$ are shown to indicate the effect of increasing resolution. The frequency in the random dimension is accurately simulated in both cases. Figure 10 shows how the simulated amplitude depends on the sample value of the rv z for $J \in \{3, 5, 6\}$. For a fixed size of the original MCS ensemble, the amplitude variance increases slightly with J . In addition, the piece-wise constant nature of the Haar basis functions causes the simulated amplitudes to be confined to a discrete set, with the number of possible amplitude values being 2^{J+1} .

Concluding Remarks

The WHa expansion of oscillatory processes has been shown to virtually eliminate the long-term inaccuracies displayed by spectral expansions. A more general multiresolution analysis of the random dimension with greater regularity should be explored to overcome the amplitude quantization exhibited by the WHa expansion.

Reference

1. Pettit, C.L., "Uncertainty Quantification in Aeroelasticity: Recent Results and Research Challenges", *Journal of Aircraft* (to appear), 2004.
2. Pettit, C.L. and Beran, P.S., "Effects of Parametric Uncertainty on Airfoil

Limit Cycle Oscillation”, *Journal of Aircraft*, Vol. 40, No. 5, Sept.-Oct. 2003, pp. 1004-1006.

3. Le Maître, O.P., Knio, O.M., Najm, H.N., and Ghanem, R.G., “Uncertainty Propagation Using Wiener-Haar Expansions”, *Journal of Computational Physics* (to appear), 2003.
4. Pettit, C.L. and Beran, P.S., “Polynomial Chaos Expansion Applied to Airfoil Limit Cycle Oscillations”, to be presented at *45th AIAA/ASME/ASCE/AHS/ASC Structures, Structural Dynamics, and Materials Conference*, Palm Springs, CA, April 2004.

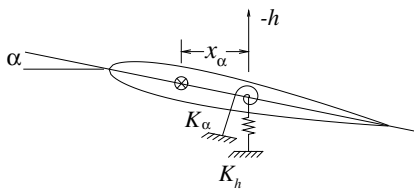


Figure 1: Two degree-of-freedom airfoil.

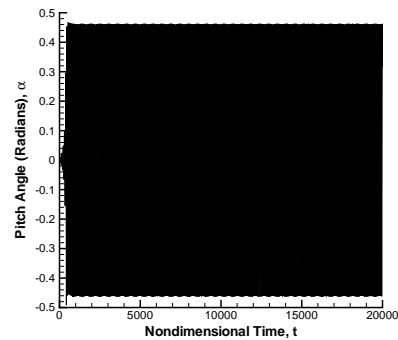


Figure 2: Baseline airfoil pitch time history.

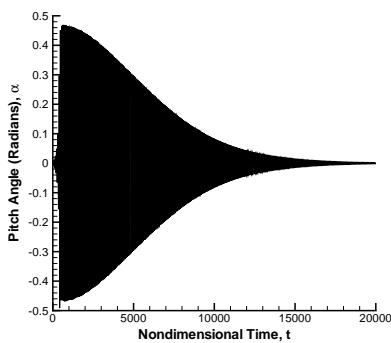


Figure 3: Airfoil pitch response simulated by WHe expansion with $P = 3$.

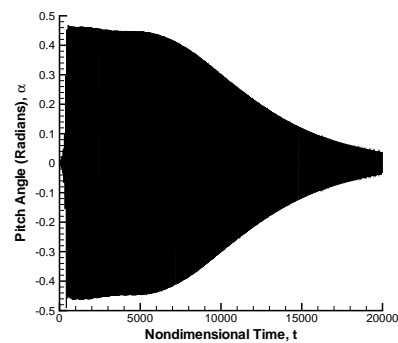


Figure 4: Airfoil pitch response simulated by WHe expansion with $P = 10$.

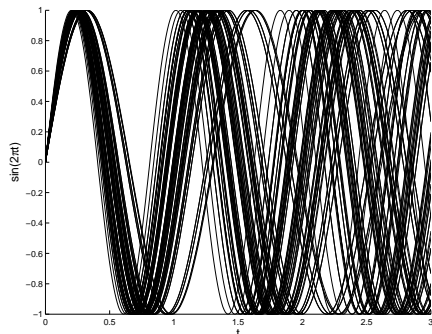


Figure 5: Fifty realizations of the sinusoidal process from $t = 0$ to $t = 3$.

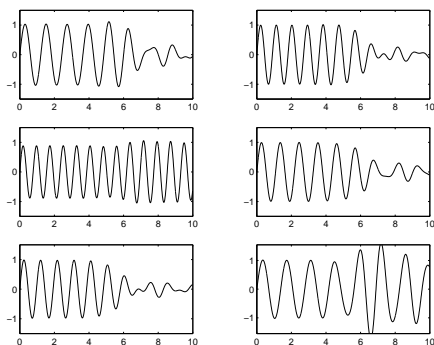


Figure 7: Six realizations of sinusoidal process's tenth-order WLe expansion from $t = 0$ to $t = 10$.

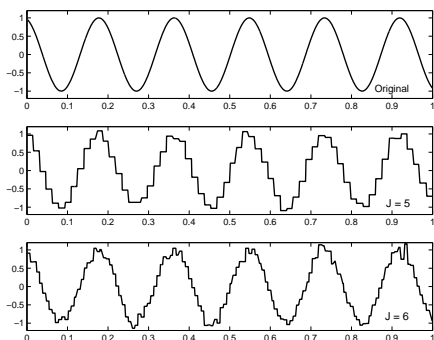


Figure 9: Observed values of the sinusoidal process at $t = 9$ plotted against the associated value of the uniform random variable.

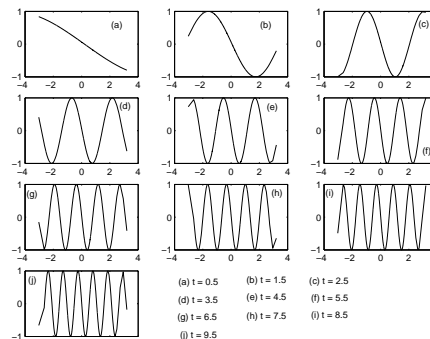


Figure 6: Plots of $x(t)$ versus ξ at $t = 0.5, 1.5, \dots, 9.5$. The abscissa, ξ , is limited by the Monte Carlo sample values.

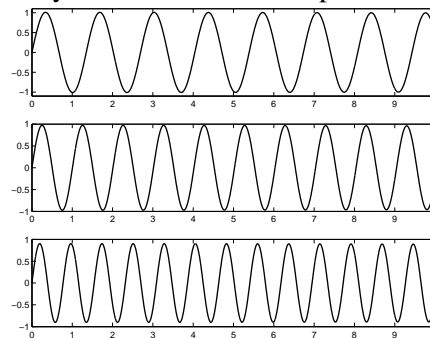


Figure 8: Three realizations of the sinusoidal process's WHa expansion with six resolution levels ($J = \max(j) = 5$) and $t = 0$ to $t = 10$.

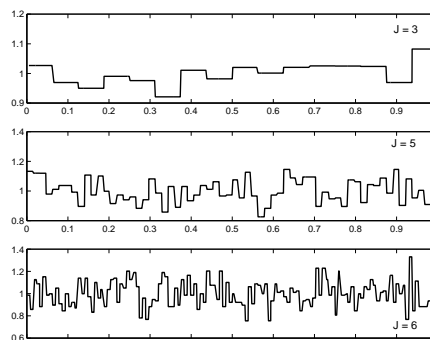


Figure 10: Observed amplitudes in the simulated sine realizations as a function of z . The top, middle, and bottom frames are for $J = \{3, 5, 6\}$, respectively.